Accepted Manuscript

Identification of new pyrrolo[2,3-*d*]pyrimidines as Src tyrosine kinase inhibitors *in vitro* active against Glioblastoma

Francesca Musumeci, Anna Lucia Fallacara, Chiara Brullo, Giancarlo Grossi, Lorenzo Botta, Pierpaolo Calandro, Mario Chiariello, Miroslava Kissova, Emmanuele Crespan, Giovanni Maga, Silvia Schenone

PII: S0223-5234(16)31041-8

DOI: 10.1016/j.ejmech.2016.12.036

Reference: EJMECH 9127

To appear in: *European Journal of Medicinal Chemistry*

Received Date: 20 September 2016

Revised Date: 14 December 2016

Accepted Date: 17 December 2016

Please cite this article as: F. Musumeci, A.L. Fallacara, C. Brullo, G. Grossi, L. Botta, P. Calandro, M. Chiariello, M. Kissova, E. Crespan, G. Maga, S. Schenone, Identification of new pyrrolo[2,3-*d*]pyrimidines as Src tyrosine kinase inhibitors *in vitro* active against Glioblastoma, *European Journal of Medicinal Chemistry* (2017), doi: 10.1016/j.ejmech.2016.12.036.

Identification of new pyrrolo[2,3-*d*]pyrimidines as Src tyrosine kinase inhibitors *in vitro* active against Glioblastoma

Francesca Musumeci, Anna Lucia Fallacara, Chiara Brullo, Giancarlo Grossi, Lorenzo Botta, Pierpaolo Calandro, Mario Chiariello, Miroslava Kissova, Emmanuele Crespan, Giovanni Maga and Silvia Schenone

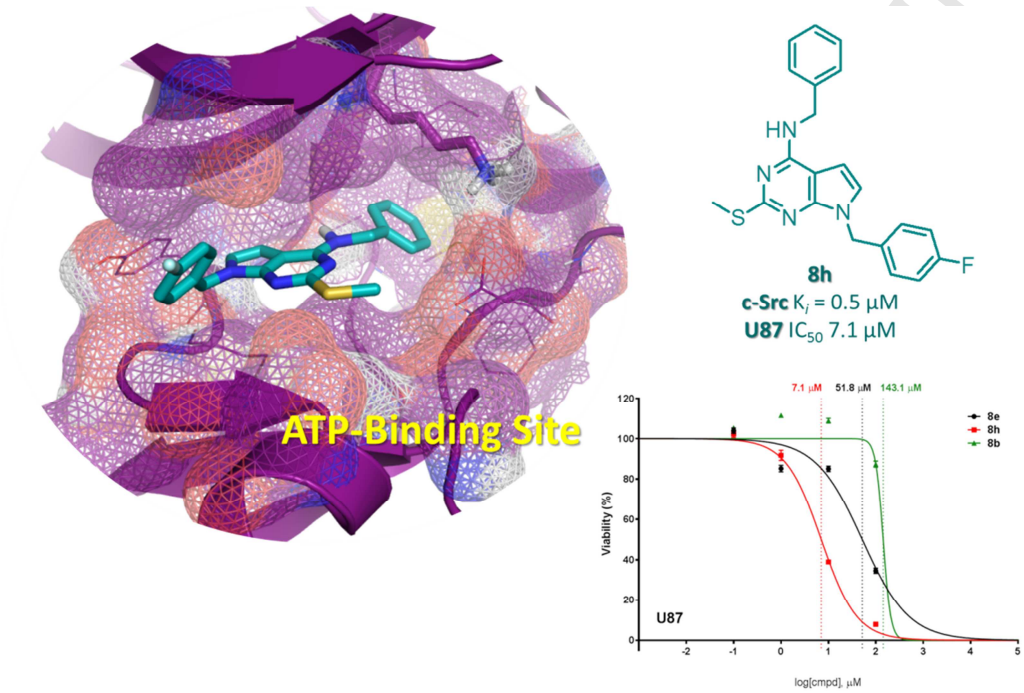

Identification of new pyrrolo[2,3-*d*]pyrimidines as Src tyrosine kinase inhibitors *in vitro* active against Glioblastoma

Francesca Musumeci[a,1], Anna Lucia Fallacara[b,1], Chiara Brullo[a], Giancarlo Grossi[a], Lorenzo Botta[c], Pierpaolo Calandro[b], Mario Chiariello[d], Miroslava Kissova[e], Emmanuele Crespan[e], Giovanni Maga[e] and Silvia Schenone[a*]

[a]Dipartimento di Farmacia, Università degli Studi di Genova, Viale Benedetto XV, 3, 16132 Genova, Italy

[b]Dipartimento di Biotecnologie, Chimica e Farmacia, Università degli Studi di Siena Via Aldo Moro 2, 53100 Siena, Italy

[c]Dipartimento di Farmacia, Università "Federico II" di Napoli, Via D. Montesano 49, 80131 Napoli, Italy

[d]Consiglio Nazionale delle Ricerche, Istituto di Fisiologia Clinica and Istituto Toscano Tumori, Core Research Laboratory, Via Fiorentina 1, 53100 Siena, Italy.

[e]Consiglio Nazionale delle Ricerche, Istituto di Genetica Molecolare, IGM-CNR, Via Abbiategrasso 207, 27100 Pavia, Italy

[1] These authors contributed equally to the publication.

Abstract

In the last few years, several pyrrolo-pyrimidine derivatives have been either approved by the US FDA and in other countries for the treatment of different diseases or are currently in phase I/II clinical trials. Herein we present the synthesis and the characterization of a novel series of pyrrolo[2,3-*d*]pyrimidines, compounds **8a-j**, and their activity against Glioblastoma multiforme (GBM). Docking studies and MM-GBSA analysis revealed the ability of such compounds to efficiently interact with the ATP binding site of Src. Enzymatic assays against a mini-panel of kinases (Src, Fyn, EGFR, Kit, Flt3, Abl, AblT315I) have been performed, showing an unexpected selectivity of our pyrrolo[2,3-*d*]pyrimidines for Src. Finally, the derivatives were tested for their antiproliferative potency on U87 GBM cell line. Compound **8h** showed a considerable cytotoxicity effect against U87 cell line with an IC_{50} value of 7.1 μM.

Keywords: pyrrolo-pyrimidines, Src, Glioblastoma, kinase inhibitors, small molecules

1. Introduction

SFKs (Src family kinases) are a family of cytoplasmic tyrosine kinases (TKs) composed of eight highly homologous members, Src, Fyn, Yes, Blk, Fgr, Hck, Lck and Lyn. They present a conserved structure which includes a N-terminal region, two Src homology domains (SH2 and SH3), a catalytic domain (SH1) and, finally, a short C-terminal tail [1]. These kinases are overexpressed or hyperactivated in several pathologies, especially in cancer [2]. Among SFKs, c-Src is involved in pathways controlling cell proliferation, migration, invasion and angiogenesis [3]. High levels of c-Src in different tumors are generally correlated with a poor prognosis. Recently, c-Src has been shown to be frequently hyperactivated or overexpressed also in Glioblastoma multiforme (GBM), a brain tumor characterized by a high degree of proliferation, angiogenesis, necrosis, and invasiveness. Src inhibition reduced GBM cell growth, viability and migration both *in vitro* and in mouse models [4].

For all these reasons, c-Src is a good therapeutic target, and many small molecules Src inhibitors have been developed for the treatment of different tumors [5]. However, because of the high homology among the catalytic domains of some cytoplasmic TKs, Src inhibitors are active also on other TKs, in particular on Bcr-Abl, a chimeric kinase present in chronic myeloid leukemia (CML) [6]. In the last ten years, three dual Src/Abl inhibitors have been approved and are currently on the market as first or second line therapy for CML. These are dasatinib, (Sprycel™, by Bristol-Myers Squibb), bosutinib, (Bosulif®, by Pfizer), and very recently, ponatinib (Iclusig®, Ariad Pharma Ltd) (**Fig. 1**) [7]. These drugs and other compounds, e.g. saracatinib (**Fig. 1**) are being tested in clinical trials, alone or in combination, for the treatment of solid malignancies.

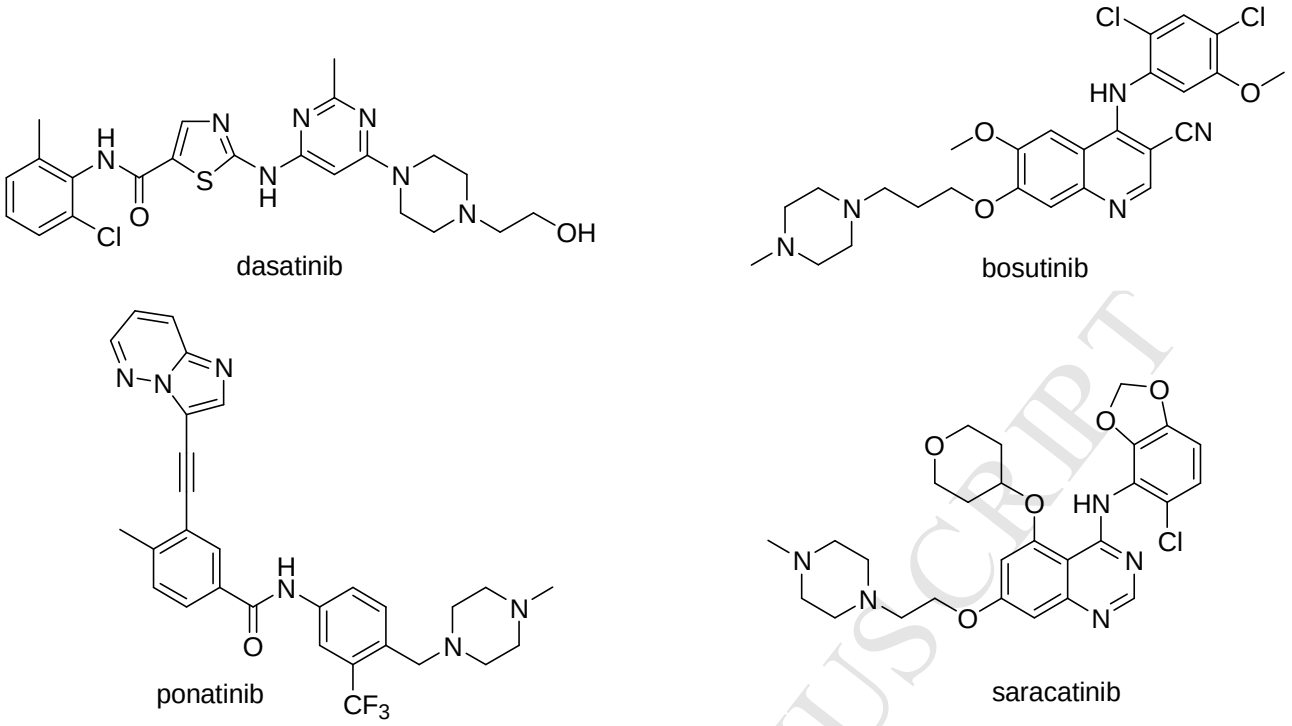

Fig. 1. Structures of dual Src/Abl inhibitors approved or in clinical trials for solid or hematologic malignancies.

Recently, different libraries of pyrazolo[3,4-*d*]pyrimidines active as SFK and/or Abl inhibitors have been synthesized [8,9]. In particular, our in house compounds **1** (**Fig. 2**) showed K_i values in the nanomolar range both in enzymatic and cell assays and possessed *in vivo* antitumor activity on xenograft models derived from different cell lines [10-12].

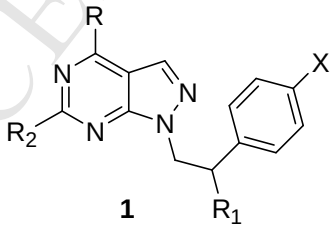

1

R = aliphatic or aromatic amino groups
R_1 = H, CH_3, Cl
R_2 = H, alkyl, thioalkyl and aminoalkyl groups
X = H, F, Cl, Br

Fig. 2. In house library of pyrazolo[3,4-*d*]pyrimidines **1**.

On the other hand, the pyrrolo[2,3-*d*]pyrimidine scaffold is being extensively investigated and in the last few years many of such compounds resulted active as kinase inhibitors. The Jak kinase inhibitors tofacitinib **2** [13], ruxolitinib **3** [14] and oclacitinib **4** [15] (**Fig. 3**) have been recently approved by the US FDA and in other countries for the treatment of rheumatoid arthritis, myelofibrosis and canine allergic dermatitis, respectively, and other similar Jak inhibitors are in clinical trials [16]. AEE788, **5** (**Fig. 3**) is a dual EGFR/VEGFR inhibitor [17,18] which has been evaluated in phase I/II clinical trials [19] for its activity in patients with recurrent or relapsed GBM. CCT128930, **6** [20] and AZD5363, **7** [21] (**Fig. 3**) inhibit Akt, a serine-threonine kinase often deregulated in tumors, such as GBM, breast and gastric cancer. AZD5363 is currently being tested in several clinical trials for the treatment of different solid malignancies [22]. Other recently published pyrrolo[2,3-*d*]pyrimidines include leucine-rich repeat kinase-2 (LRRK2) [23], 3-phosphoinositide dependent protein kinase-1 (PDK1) [24], Aurora kinase [25], multiple TK receptors (VEGFR, EGFR, PDGFR) [26, 27] and Bruton's tyrosine kinase (Btk) inhibitors [28].

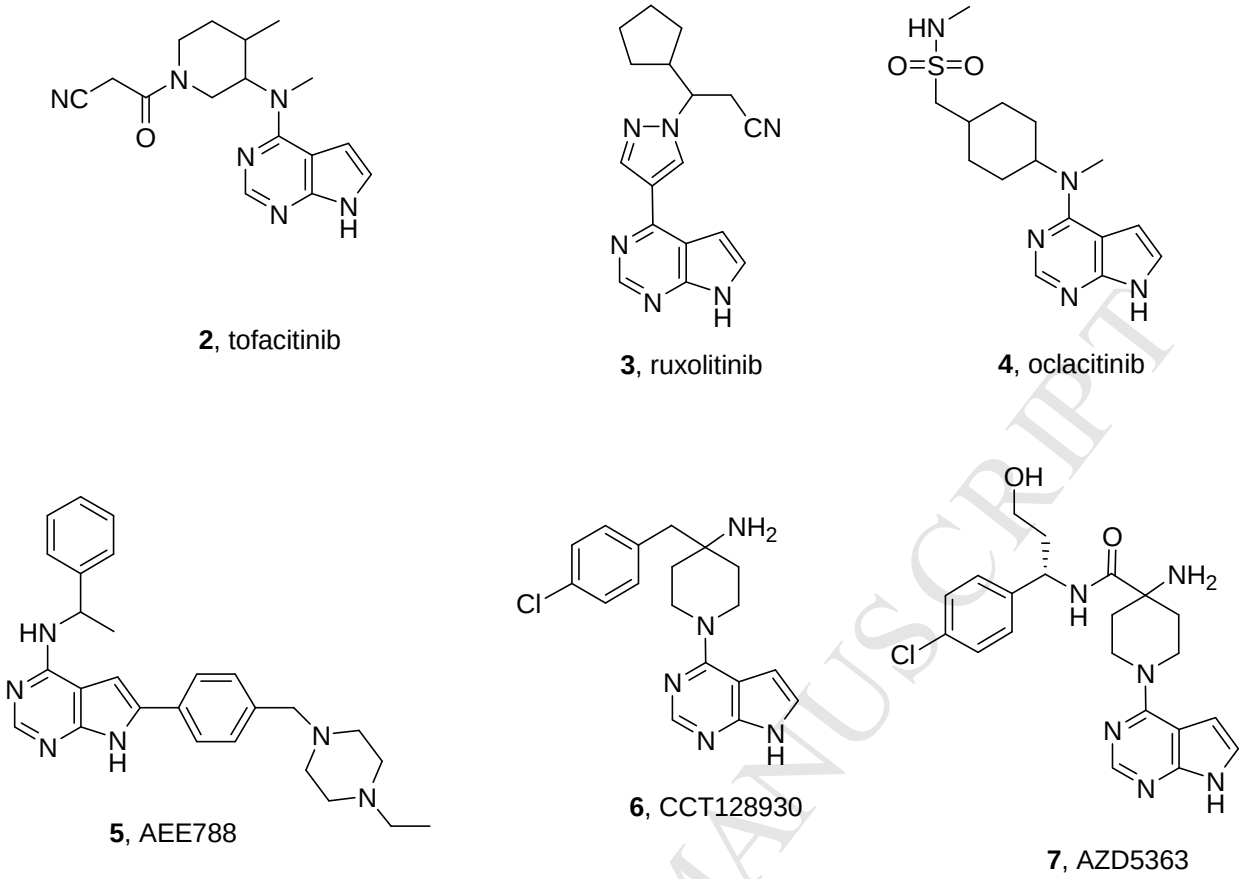

Fig. 3. Pyrrolo[2,3-*d*]pyrimidine kinase inhibitors.

Interestingly, some recently appeared derivatives are also active on Src [29-31].

On the basis of this knowledge and with the aim of investigating if the deaza-isosteres of in house inhibitors **1** maintain the activity on Src both in enzymatic and in cell assays, we decided to synthesize a family of pyrrolo[2,3-*d*]pyrimidines **8** (**Fig. 4**), and to test them on Src in enzymatic assays and as antiproliferative agents on a specific cancer cell line. Some of compounds **8** are strictly correlated with their pyrazolo[3,4-*d*]pyrimidine analogues **1** bearing a C2 thiomethyl group, a C4 amino group, and a N7 2-chloro-2-phenylethyl chain, whereas other derivatives are substituted in N7 with a benzylic chain, more easily accessible from a synthetic point of view.

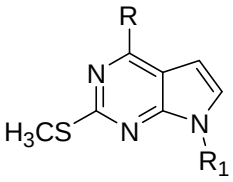

8

R = amino groups
R_1 = $CH_2CHClC_6H_5$, $CH_2C_6H_4$-*p*F

Fig. 4. General structure of pyrrolo[2,3-*d*]pyrimidines **8**.

2. Results and Discussion

2.1. Synthesis of pyrrolo[2,3-d]pyrimidine derivatives

The synthesis of compounds **8a-c** was performed starting from 6-amino-2-(methylthio)pyrimidin-4(3*H*)-one **9**, prepared following the procedure reported by Baker and coll. [32]. Compound **9** was cyclized using an aqueous solution of chloroacetaldehyde in a microwave open vessel apparatus to obtain 2-(methylthio)-7*H*-pyrrolo[2,3-*d*]pyrimidin-4-ol **10** in a higher yield compared to the literature method [33]. Then compound **10** was chlorinated in C4 to give 4-chloro-2-(methylthio)-7*H*-pyrrolo[2,3-*d*]pyrimidine **11** following a literature method [33]. Intermediate **11** was alkylated in N7 using 2-bromo-1-phenylethanone at room temperature in the presence of sodium hydride to obtain compound **12**. The latter was reduced to **13** with sodium borohydride in a mixture of THF and water. Intermediate **13** was in turn treated with the Vilsmeier complex ($POCl_3$/DMF, 1:1) in CH_2Cl_2 at reflux for 8h to obtain compound **14**, bearing a 2-chloro-2-phenyethyl chain in N7. Finally, reaction of **14** with the suitable anilines in absolute ethanol at reflux for 3-5h gave the desired compounds **8a,b** in good yields, while compound **8c** was obtained by treating **14** with an excess of benzylamine in anhydrous toluene at room temperature for 24h (**Scheme 1**).

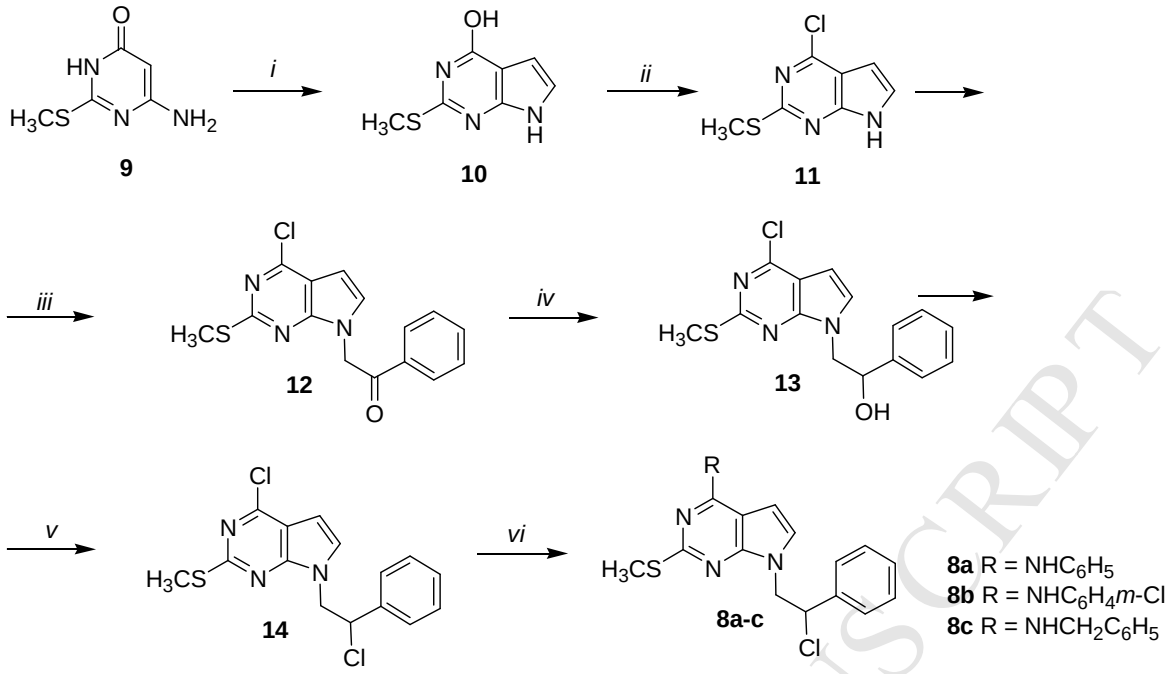

Scheme 1. Synthetic route for the preparation of **8a-c**. Reagents and conditions: (i) Chloroacetaldehyde (50% aq. solution), AcONa, H_2O, MW 100 W, 80 °C, 2 min. (ii) $POCl_3$, TEA, 130 °C, 4h. (iii) NaH, anhyd. DMF, 0 °C, 20 min, then 2-bromo-1-phenylethanone, from 0 °C to rt, 18h. (iv) $NaBH_4$, THF, H_2O, 0 °C, then rt, 3h. (v) $POCl_3$/DMF, CH_2Cl_2, reflux, 8h. (vi) Method A: anilines, abs. EtOH, reflux, 5h (to obtain compounds **8a,b**)*;* Method B: benzylamine, anhyd. toluene, rt, 24h (to obtain compound **8c**).

The synthesis of compounds **8d-j** was performed starting from 4-chloro-2-(methylthio)-7*H*-pyrrolo[2,3-*d*]pyrimidine **11**, which was alkylated in N7 with sodium hydride and 4-fluorobenzyl chloride in anhydrous acetonitrile at 50 °C for 2h to give 4-chloro-7-(4-fluorobenzyl)-2-(methylthio)-7*H*-pyrrolo[2,3-*d*]pyrimidine **15**. The compound was treated with the suitable amine in DMSO at 90-130 °C to obtain the desired compounds **8d-j** (**Scheme 2**).

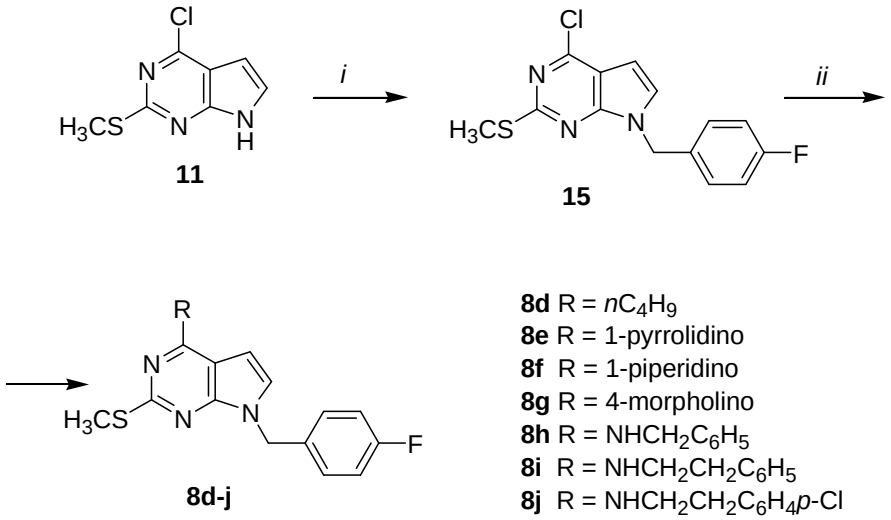

Scheme 2. Synthetic route for the preparation of **8d-j**. Reagents and conditions: (i), NaH, anhyd. CH_3CN, 4-fluorobenzyl chloride**,** 50 °C, 2h. (ii) amines, DMSO, 90-130 °C, 3-5h.

2.2 Molecular Modeling Studies

A molecular docking protocol has been employed in order to evaluate the ability of the new synthesized compounds **8a-j** to interact with the ATP-binding site of c-Src kinase. For this purpose, the X-ray crystal structure of Src in a complex with a pyrazolo[3,4-*d*]pyrimidine derivative, **11V**, (PDB code: 4O2P) [11], previously solved and reported by us, was used for computational studies. The 4O2P X-ray structure was shown to contain two protein molecules within the crystallographic cell unit, referred as chain A and chain B, respectively.

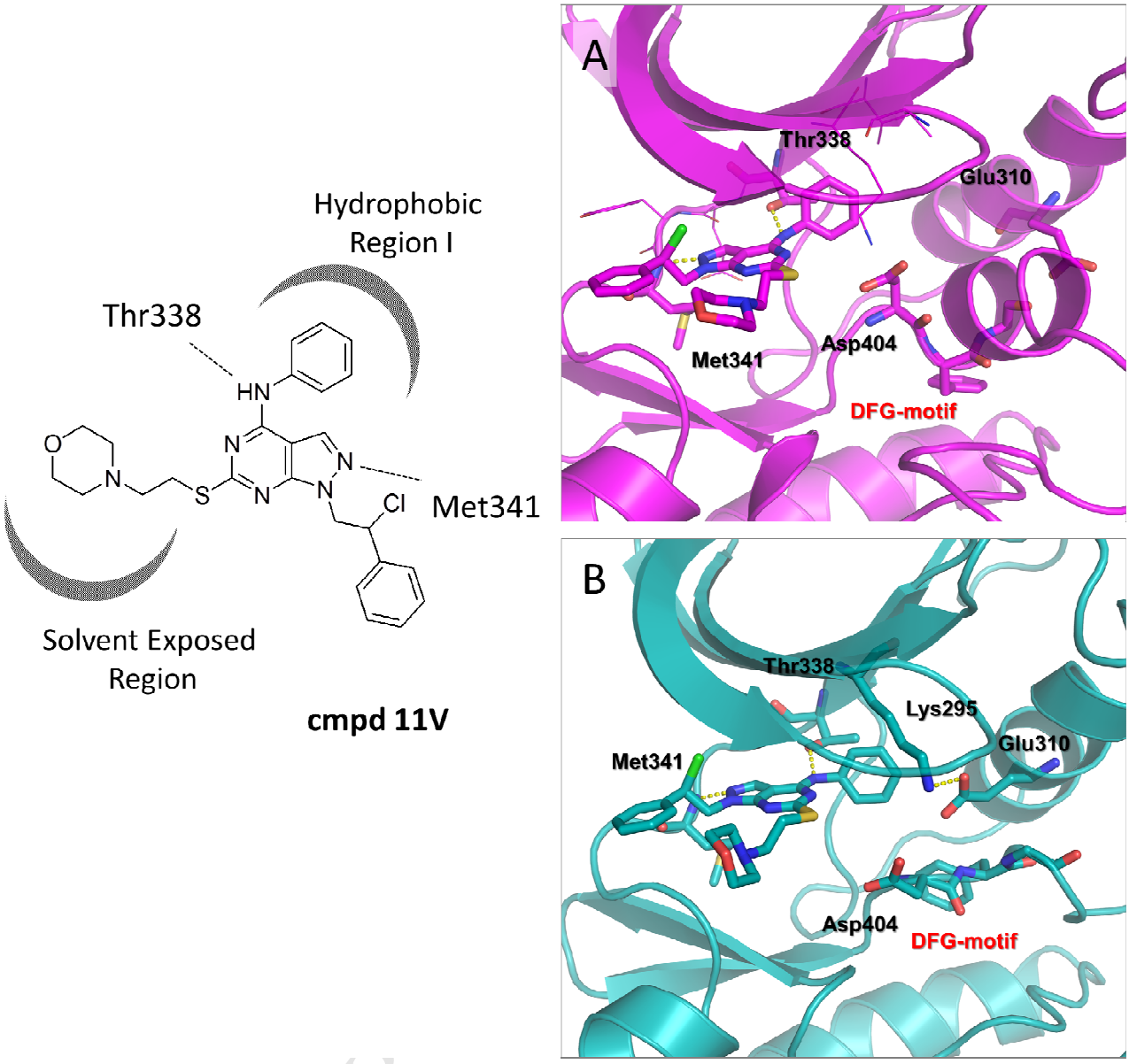

Fig 5. *Left)* Schematic representation of **11V** ligand's interactions within the ATP-binding site of c-Src; *Right)* Binding mode of **11V** in 4O2P crystal structure: panel A and panel B show chain A and chain B, respectively. DFG-motif and Glu310 are displayed as sticks. Hydrogen bonds are reported as yellow dashes.

Many conformational differences have been observed between the two chains especially in the αC-helix and in the rearrangement of the activation loop (**Fig. 5**). The ligand **11V** was found to have a similar binding pose in both chains, but the protein binds the compound assuming two different conformations. Indeed, in chain A (**Fig. 5A**) the Glu310 side chain is turned away from the ATP-

binding site and exposed to the solvent, resulting in a rotation of the αC-helix usually observed in the inactive conformation of the Src-family members. The chain A conformation appears very similar to the ones of the inhibited enzyme phosphorylated on Tyr527 (PDB code: 2SRC [34]; PDB code: 2PTK [35]). Moreover, the N-terminal amino acids of the activation loop are arranged in a three-turns α-helix that resemble the 2SRC structure. On the contrary, in the chain B Glu310 displays its side chain projected toward the ATP-binding site forming a salt bridge with Lys295 (**Fig. 5B**). Another important feature is represented by the orientation of the Asp404 belonging to the DFG motif: in chain A the side chain of Asp404 creates a steric hindrance which reduces the size of the hydrophobic pocket I, hindering the binding of molecules with an elongated shape. Taking into account the structural differences between the two structures and the conformational plasticity of c-Src kinase in the presence of small molecules, both chains have been used for molecular modeling simulations.

Docking studies have been performed by means of the docking software Glide [36]. Both chain A and B have been prepared for the docking procedure by using the Protein Preparation Wizard protocol [37]. The missing residues were replaced and all the loops refined according to a procedure already reported [11].

The reliability of the docking protocol was assessed by simulating the interactions between **11V** and c-Src and then comparing the modelled complexes with the experimental structures. As a result, the program was able to reproduce in both the chains the binding mode of **11V**.

Compounds **8a-j** were drawn, minimized and finally docked into the catalytic site of Src. All the binding poses have been submitted to a MM-GBSA rescoring. After rescoring, the best docking poses have been analysed. The best binding modes, in terms of both energies and reliability of the poses, have been found for compounds **8a-c**, whose molecular structures closely resemble the one of the pyrazolo[3,4-*d*]pyrimidine **11V**. In compounds **8a-c**, bearing a 2-chloro-2-phenylethyl chain in N7, the C4 substituent kept contacts with the hydrophobic region 1 (HR1) in the ATP-binding site of Src establishing a hydrogen bond through the NH group with the Thr338 side chain.

Moreover, a cation-π interaction occurs between Lys295 and the anilino ring maintaining the ligand stable in its binding mode (**Fig. 6A**).

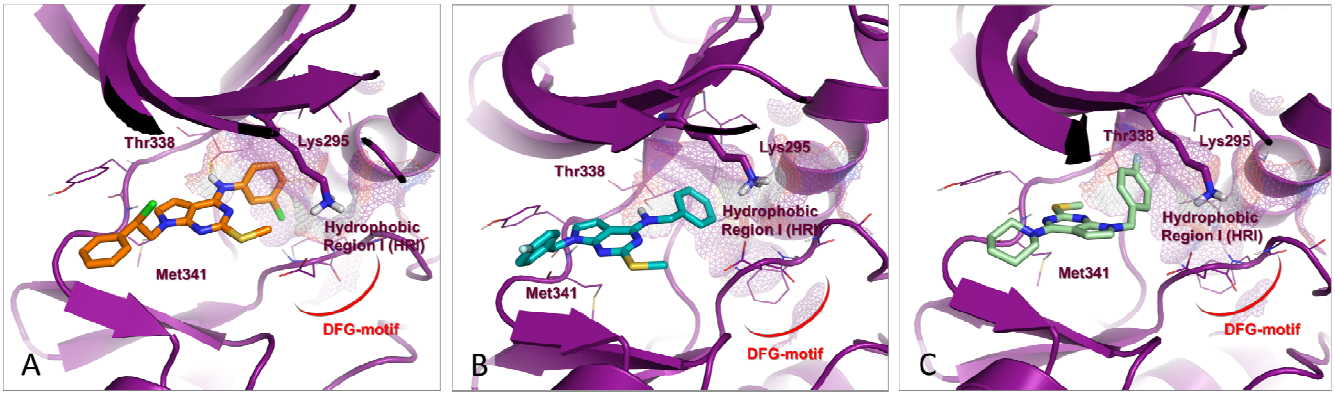

Fig 6. Best predicted docking poses of compounds **8b** (orange, panel A), **8h** (deep teal, panel B) and **8e** (pale green, panel C) within the ATP binding site of 4O2P crystal structure chain B.

Compound **8b** has been scored as the best compound (**Table S2**) of the series thanks to the presence of the chlorine atom in *meta* position on the R substituent which interacts with Asp404 and Phe405 belonging to the DFG-motif. For compounds **8a-c** similar results were obtained in both the chains. On the other hand, some differences have been observed for derivatives **8h-j** between chain A and B. In chain A, because of the conformation of the Asp404 which partially occupies the entrance of the HR1, the size of the binding site is reduced and this feature does not allow the program to fit the ligands into the ATP-binding site with a unique and rational binding pose. Conversely, in chain B reasonable binding modes with high docking scores were found. In particular, after rescoring, **8h** has been predicted to have a good ΔG of binding (**Table S2**) forming a cation-π interaction with Lys295 and profitable hydrophobic contacts with HRI (**Fig. 6B**). The presence of a substituent in C4 position with a longer spacer seems to be unfavourable in the case of **8h**, if compared with **8b**, because of steric hindrance which does not allow the formation of the hydrogen bond between the NH group and the side chain of Thr338. The ligand pose results shifted toward the solvent with hydrophobic interactions, with HR1 mostly stabilizing the binding mode. The negative effect of a long C4 substituent is more evident in the case of compounds **8i** and **8j** which partially come out

from the site. Derivatives **8d-g** present a characteristic binding mode, probably because of the more polar nature of their R substituents, with the N7 group projecting into the HR1 and the R substituent being solvent exposed (**Fig. 6C**). Moreover, the pyrrolo-pyrimidine core was found rotated of 180 degrees with the SCH_3 group projecting toward the hinge region.

As a final consideration, despite the binding poses of compounds **8a-j** present common features with those of the ligand **11V**, pyrrolo-pyrimidines lack the nitrogen atom which usually interacts with the backbone of Met341 in the pyrazolo[3,4-*d*]pyrimidine analogues. The absence of this important point of contact with the hinge region makes our pyrrolo[2,3-*d*]pyrimidines less active than their pyrazolo counterpart, but they open the way to the study of a new promising scaffold which could be further optimized.

2.3. Enzymatic Assays

All synthesized compounds were initially tested in a cell free assay (see Experimental Section) to evaluate their affinity toward isolated c-Src (**Table 1**).

In agreement with our computational studies, **8b** resulted one of the best compounds of our small library of pyrrolo[2,3-*d*]pyrimidines, showing a good inhibitory effect of the enzymatic activity with a K_i value of 0.7 µM. As expected, **8c**, which has a longer side chain as R substituent, or **8a**, which lacks the *m*Cl substituent, did reduce the activity of the enzyme in a less efficient way than **8b**. In the series **8d-j** the substitution of the 2-chloro-2-phenylethyl side chain in R_1 with a shorter 4-fluoro-benzyl group, which lacks the bulky Cl atom, gives the possibility to the compounds with a longer R substituent to better accommodate into the ATP binding cleft and go deeply into the HR1. This is confirmed by the fact that **8h** also showed a good inhibitory activity against c-Src (0.5 µM), despite the presence of a long benzyl group as R substituent. In general, for all two series, it was observed that increasing the length of the linker at C4 position caused a high reduction of the inhibitory power against c-Src (compare **8c** with **8b** and **8j** with **8h**). On the other hand, compound

8d, bearing a *n*C_4H_9 substituent in C4 and a 4-fluoro-benzyl chain in N7, showed to be too small for effectively bind the ATP cleft of Src (K_i = 3 μM).

Table 1: Structures and inhibitory activity of compounds **8a-j**.

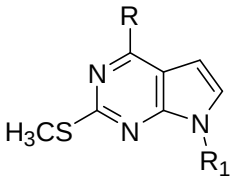

Cmpd	R	R_1	Src (K_i, μM)[a]	U87 (IC_{50}, μM)
8a	NHC_6H_5	$CH_2CHClC_6H_5$	1.5±0.10	27.4±0.16
8b	NHC_6H_4-*m*Cl	$CH_2CHClC_6H_5$	0.7±0.20	143.1±0.20
8c	$NHCH_2C_6H_5$	$CH_2CHClC_6H_5$	6.0±0.08	50.7±0.18
8d	*n*C_4H_9	$CH_2C_6H_4$-*p*F	3.0±0.10	20.7±0.38
8e	1-pyrrolidino	$CH_2C_6H_4$-*p*F	2.0±0.30	51.8±0.21
8f	1-piperidino	$CH_2C_6H_4$-*p*F	2.5±0.30	50.7±0.42
8g	4-morpholino	$CH_2C_6H_4$-*p*F	4.7±0.20	20.3±0.15
8h	$NHCH_2C_6H_5$	$CH_2C_6H_4$-*p*F	0.5±0.06	7.1±0.16
8i	$NHCH_2CH_2C_6H_5$	$CH_2C_6H_4$-*p*F	0.8±0.04	13.3±0.16
8j	$NHCH_2CH_2C_6H_4$-*p*Cl	$CH_2C_6H_4$-*p*F	5.0±0.10	46.1±0.08

[a]Values are the mean of at least two experiments.

The compounds have been also tested on Fyn, another member of SFKs, and showed a certain degree of activity, probably due to the similarity among the members of this family of kinases. The most active compound is **8i** which possesses a K_i value of 2 μM on this enzyme.

On the other hand, the compounds resulted inactive when tested on a small panel of kinases, including c-Kit, Abl, AblT315I, Flt3 and EGFR, demonstrating a degree of selectivity toward c-Src.

2.4 Cytotoxicity Assays on U87 GB cell line

The compounds have been successively tested on U87 GB cell line, that has been chosen because of Src involvement in this aggressive tumor [38].

The most active compound was **8h**, with an IC_{50} value of 7.1 μM after 72h, while the other derivatives resulted less active with IC_{50} values higher than 10 μM (**Fig. 7**).

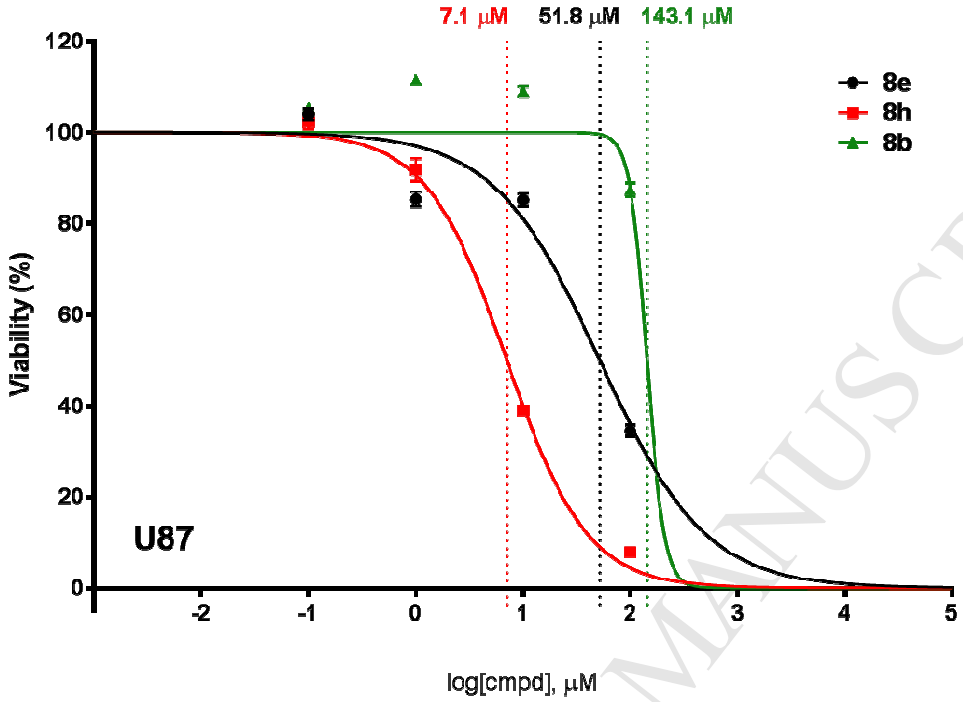

Fig. 7. Viability of U87 cell line evaluated at 72h is reported for the most active compound **8h** and for **8b** and **8e** as examples of less active compounds of each series.

3. Conclusions

A series of pyrrolo[2,3-*d*]pyrimidines has been synthesized and tested for their activity against c-Src. Molecular docking studies together with a MM-GBSA rescoring approach revealed our compounds possess profitable features for the binding to the catalytic site of c-Src, being able to act as ATP-competitive inhibitors of the enzyme. Compounds **8a-j** have been tested on a small panel of kinases. As a result, our pyrrolo[2,3-*d*]pyrimidines demonstrated a certain selectivity for c-Src, since they did not show any activity against other tyrosine kinases, with the only exception of **8i** which turned out moderately active against Fyn.

The compounds have been finally tested *in vitro* for their cytotoxicity on U87 GB cell line and **8h** demonstrated to be active with an IC_{50} value of 7.1 μM.

The inadequacy of the current therapies against GBM raises the need of new drugs able to inhibit the growth of this aggressive tumor. In this contest, our pyrrolo[2,3-*d*]pyrimidine derivatives stand as a new promising scaffold with a good potency against GBM and therefore worthy of further investigation.

4. Experimental

4.1 Chemistry. Starting materials were purchased from Aldrich-Italia (Milan, Italy). Melting points were determined with a Büchi 530 apparatus and are uncorrected. IR spectra were measured in KBr with a Perkin-Elmer 398 spectrophotometer. ^{1}H and ^{13}C NMR spectra were recorded on a Varian Gemini 200 (200 MHz) instrument. Chemical shifts are reported as δ (ppm) relative to TMS as the internal standard, *J* in Hz. ^{1}H patterns are described using the following abbreviations: s = singlet, d = doublet, t = triplet, q = quartet, q = quintet, s = sextet, m = multiplet, and br s = broad singlet. TLC was carried out using Merck TLC plates silica gel 60 F254. Chromatographic purifications were performed on columns packed with Florisil®, 100-200 mesh, or with Fluka silica gel 60 Å, 220-440 mesh, for flash technique. Analyses for C, H, N and S were within ±0.3% of the theoretical value. Mass spectra (MS) data were obtained using an Agilent 1100 LC/MSD VL system (G1946C) with a 0.4 mL/min flow rate using a binary solvent system of 95:5 methanol/water. UV detection was monitored at 254 nm. MS were acquired in positive and negative modes, scanning over the mass range 50-1500. The following ion source parameters were used: drying gas flow, 9 mL/min; nebulizer pressure, 40 psig; drying gas temperature, 350 °C. All target compounds possessed a purity of ≥95% as verified by elemental analyses by comparison with the theoretical values.

Microwave apparatus: CEM Discover (CEM Corporation, Matthews, NC, USA), single-mode microwave oven, max emitted power 300 Watt, temperature control by optical fiber, magnetic stirring of the sample, air cooling system.

4.1.1 2-(Methylthio)-7*H*-pyrrolo[2,3-*d*]pyrimidin-4-ol (10).

Chloroacetaldehyde (50% aqueous solution, 1 mL, 7.87 mmol) was added to a suspension of 6-amino-2-(methylthio)pyrimidin-4(3*H*)-one **9** (0.5 g, 3.18 mmol) and sodium acetate (0.88 g, 10.69 mmol) in water (12.5 mL) and the mixture was heated at 80 °C for 2 min in a microwave oven (open vessel mode, 100 W). After cooling to room temperature, acetone (3 mL) was added and the obtained solid was filtered. Grey solid (yield 71%, lit. 55%), constituted by a mixture of the C4 keto enolic forms, as shown by IR and ^{1}H NMR data [33]. Mp: 265-267 °C. ^{1}H NMR (DMSO): δ 3.26 (s, 3H, SCH_3), 7.61-7.65 (m, 1H, H-5), 7.75-7.90 (m, 1H, H-6), 9.59 (br s, 1H disappears with D_2O), 9.92 (br s, 1H disappears with D_2O). IR (KBr) cm^{-1}: 3330-2900 (OH), 3220 (NH), 1667 (C=O). MS: *m/z* $[M+1]^+$ 182. Anal. calcd. for $C_7H_7N_3OS$, C 46.39, H 3.89, N 23.19, S 17.69, found C 46.51, H 3.96, N 23.15, S 17.68.

4.1.2 4-Chloro-2-(methylthio)-7*H*-pyrrolo[2,3-*d*]pyrimidine (11).

$POCl_3$ (5 mL, 53.7 mmol) and triethylamine (0.2 mL, 1.43 mmol) were added to 2-(methylthio)-7*H*-pyrrolo[2,3-*d*]pyrimidin-4-ol **10** (0.10 g, 0.55 mmol); the mixture was heated at 130 °C for 4h and then cooled to room temperature. The excess of $POCl_3$ was removed by distillation under reduced pressure. Ice was then carefully added to the residue and the suspension was extracted with diethyl ether (3 x 20 mL). The organic phase was washed with H_2O (10 mL), dried on $MgSO_4$, filtered and concentrated under reduced pressure. The crude was purified by column chromatography (Florisil®, 100-200 mesh), using diethyl ether as the eluent to afford the pure product 4-chloro-2-(methylthio)-7*H*-pyrrolo[2,3-*d*]pyrimidine (77%, lit. 43%) [33]. Mp: 207-209 °C. ^{1}H NMR ($CDCl_3$): δ 2.67 (s, 3H, SCH_3), 6.56-6.59 (m, 1H, H-5), 7.21-7.23 (m, 1H, H-6). IR (KBr) cm^{-1}: 3412 (NH), 3122 (CH), 1614 (C=C). MS: *m/z* $[M+1]^+$ 201. Anal. calcd. for $C_7H_6N_3ClS$, C 42.11, H 3.03, N 21.05, S 16.06, found C 42.29, H 3.38, N 21.14, S 16.36.

4.1.3 2-[4-Chloro-2-(methylthio)-7*H*-pyrrolo[2,3-*d*]pyrimidin-7-yl]-1-phenylethanone (12).

Sodium hydride (60% dispersion in mineral oil, 0.04 g, 1 mmol) was added in small portions at 0 °C to a solution of 4-chloro-2-(methylthio)-7*H*-pyrrolo[2,3-*d*]pyrimidine **11** (0.2 g, 1 mmol) in anhydrous DMF and the mixture was stirred at room temperature for 20 min. Then 2-bromo-1-phenylethanone (0.3 g, 1 mmol) was added dropwise at 0 °C and the reaction was stirred at room temperature for 18h. Then the mixture was poured into water (20 mL) and extracted with ethylacetate (3 x 10 mL); the organic phases were washed with water (2 x 10 mL), dried on $MgSO_4$, filtered and concentrated under reduced pressure. The crude was purified by column chromatography (Silica gel 220-440 mesh), using CH_2Cl_2 as the eluent to afford the pure product as a white solid (47%). Mp: 157-159 °C. ^{1}H NMR ($CDCl_3$): δ 2.65 (s, 3H, SCH_3), 5.65 (s, 2H, CH_2N), 6.60 (d, *J* = 3.6, 1H, H-5), 7.11 (d, *J* = 3.6, 1H, H-6), 7.52-7.56, 7.64-7.67 and 8.03-8.05 (3m, 5H Ar). IR (KBr) cm^{-1}: 1694 (C=O). MS: *m/z* $[M+1]^+$ 319. Anal. calcd. for $C_{15}H_{12}N_3OClS$, C 56.69, H 3.81, N 13.22, S 10.09, found C 56.65, H 3.83, N 12.97, S 10.07.

4.1.4 2-[4-Chloro-2-(methylthio)-7*H*-pyrrolo[2,3-*d*]pyrimidin-7-yl]-1-phenylethanol (13).

A solution of sodium borohydride (0.26 g, 6.9 mmol) in water (1 mL) was slowly added at 0 °C to a solution of 2-[4-chloro-2-(methylthio)-*7H*-pyrrolo[2,3-*d*]pyrimidin-7-yl]-1-phenylethanone **12** (0.31 g, 1 mmol) in THF (6 mL), and the reaction was stirred at room temperature for 3h. Then the mixture was poured in water (20 mL) and extracted with diethyl ether (3 x 10 mL); the organic phases were washed with water (2 x 10 mL), dried on $MgSO_4$, filtered and concentrated under reduced pressure to obtain an oil which crystallized by adding a 1:1 mixture of ethylic ether and petroleum ether (bp 40-60 °C) to give a white solid (69%). Mp: 157-159 °C. ^{1}H NMR ($CDCl_3$): δ 2.65 (s, 3H, SCH_3), 3.91 (br s, 1H, OH disappears with D_2O), 4.32-4.64 (m, 2H, CH_2N), 5.10-5.25 (m, 1H, CHOH), 6.48 (d, *J* = 3.6, 1H, H-5), 7.03 (d, *J* = 3.6, 1H, H-6), 7.23-7.47 (m, 5H Ar). IR (KBr) cm^{-1}: 3500-3200 (OH). MS: *m/z* $[M+1]^+$ 321. Anal. calcd. for $C_{15}H_{14}N_3OClS$, C 56.33, H 4.41, N 13.14, S 10.03, found C 56.08, H 4.73, N 13.04, S 9.98.

4.1.5 4-Chloro-7-(2-chloro-2-phenylethyl)-2-(methylthio)-7*H*-pyrrolo[2,3-*d*]pyrimidine (14).

The Vilsmeier complex, previously prepared from $POCl_3$ (1.65 mL, 17.6 mmol) and DMF (1.28 g, 17.6 mmol) was added to a suspension of 2-[4-chloro-2-(methylthio)-7*H*-pyrrolo[2,3-*d*]pyrimidin-7-yl]-1-phenylethanol **13** (0.56 g, 1.76 mmol) in CH_2Cl_2 (10 mL). The mixture was refluxed for 8h. After cooling to room temperature, the mixture was washed with H_2O (2 x 20 mL), dried on $MgSO_4$, filtered, and concentrated under reduced pressure. The crude oil was purified by column chromatography (Silica gel 220-440 mesh), using diethyl ether as the eluent, to afford the pure product as a white solid (92%). Mp: 87-88 °C. ^{1}H NMR ($CDCl_3$): δ 2.65 (s, 3H, SCH_3), 4.66-4.80 (m, 2H, CH_2N), 5.29-5.34 (m, 1H, CHCl), 6.47 (d, *J* = 3.6, 1H, H-5), 6.99 (d, *J* = 3.6, 1H, H-6), 7.22-7.50 (m, 5H Ar). MS: *m/z* $[M+1]^+$ 339. Anal. calcd. for $C_{15}H_{13}N_3Cl_2S$, C 53.26, H 3.87, N 12.42, S 9.48, found C 53.23, H 3.81, N 12.18, S 9.15.

4.1.6 General procedure for compounds 8a,b.

The appropriate aniline (2 mmol) was added to a solution of 4-chloro-7-(2-chloro-2-phenylethyl)-2-(methylthio)-7*H*-pyrrolo[2,3-*d*]pyrimidine **14** (0.33 g, 1 mmol) in absolute ethanol (10 mL) and the reaction mixture was stirred at reflux for 5h. After cooling, a solid precipitated. It was filtered, washed with H_2O, and recrystallized from absolute ethanol (10 mL) to give the final products as white solids.

4.1.6.1 7-(2-Chloro-2-phenylethyl)-2-(methylthio)-*N*-phenyl-7*H*-pyrrolo[2,3-*d*]pyrimidin-4-amine (8a). Yield 66%, mp: 157-159 °C. ^{1}H NMR ($CDCl_3$): δ 2.65 (s, 3H, SCH_3), 4.72-5.22 (m, 2H, CH_2N), 5.39-5.66 (m, 1H, CHCl), 7.00-7.76 (m, 12H, H-5 + H-6 + 10Ar), 8.40 (br s, 1H, NH disappears with D_2O). IR (KBr) cm^{-1}: 3000-2830 (NH). ^{13}C NMR (MeOD): δ 168.96, 150.48, 146.94, 141.15, 138.23, 129.39, 129.08, 128.86, 127.54, 124.04, 123.66, 120.80, 101.88, 100.01, 60.17, 53.07, 14.82. MS: *m/z* $[M+1]^+$ 396. Anal. calcd. for $C_{21}H_{19}N_4ClS$, C 63.87, H 4.85, N 14.19, S 8.12, found C 63.81, H 4.62, N 14.38, S 7.99.

4.1.6.2 *N*-(3-Chlorophenyl)-7-(2-chloro-2-phenylethyl)-2-(methylthio)-7*H*-pyrrolo[2,3-*d*]pyrimidin-4-amine (8b). Yield 61%, mp: 147-149 °C. ^{1}H NMR ($CDCl_3$): δ 2.66 (s, 3H, SCH_3), 4.64-5.23 (m, 2H, CH_2N), 5.41-5.67 (m, 1H, CHCl), 7.00-7.81 (m, 11H, H-5 + H-6 + 9Ar), 9.76 (br s, 1H, NH disappears with D_2O). IR (KBr) cm^{-1}: 3000-2800 (NH). ^{13}C NMR (MeOD): δ 168.96, 150.48, 146.94, 144.13, 138.23, 134.43, 130.17, 129.39, 128.86, 127.54, 124.04, 122.58, 120.89, 120.18, 101.88, 100.01, 60.17, 53.07, 14.82. MS: *m/z* $[M+1]^+$ 430. Anal. calcd. for $C_{21}H_{18}N_4Cl_2S$, C 58.74, H 4.23, N 13.05, S 7.47, found C 58.76, H 4.37, N 13.25, S 7.11.

4.1.7 *N*-Benzyl-7-(2-chloro-2-phenylethyl)-2-(methylthio)-7*H*-pyrrolo[2,3-*d*]pyrimidin-4-amine (8c).

Benzylamine (0.4 g, 4 mmol) was added to a solution of 4-chloro-7-(2-chloro-2-phenylethyl)-2-(methylthio)-7*H*-pyrrolo[2,3-*d*]pyrimidine **14** (0.3 g, 1 mmol) in anhydrous toluene (5 mL) and the mixture was stirred at room temperature for 24h. Then, the organic phase was washed with H_2O (2 x 10 mL), dried on $MgSO_4$, and concentrated under reduced pressure. The crude oil was purified by column chromatography (Silica gel 220-440 mesh), using diethyl ether as the eluent. The obtained oil crystallized as a yellow solid by adding a 1:1 mixture of diethyl ether and petroleum ether (bp 40-60 °C) (81%). Mp: 106-107 °C. ^{1}H NMR ($CDCl_3$): δ 2.65 (s, 3H, SCH_3), 4.65-4.71 (m, 4H, CH_2N + CH_2Ar), 5.05 (br s, 1H, NH disappears with D_2O), 5.33-5.35 (m, 1H, CHCl), 6.45 (d, *J* = 3.6, 1H, H-5), 6.96 (d, *J* = 3.6, 1H, H-6), 7.18-7.50 (m, 10H Ar). IR (KBr) cm^{-1}: 3100-2900 (NH). ^{13}C NMR (MeOD): δ 169.80, 153.68, 148.47, 139.85, 138.23, 129.39, 128.86, 128.43, 127.59, 127.54, 126.92, 124.04, 103.94, 100.01, 60.17, 53.07, 43.38, 14.82. MS: *m/z* $[M+1]^+$ 410. Anal. calcd. for $C_{22}H_{21}N_4ClS$, C 64.61, H 5.18, N 13.70, S 7.84, found C 64.38, H 5.08, N 13.87, S 7.78.

4.1.8 4-Chloro-7-(4-fluorobenzyl)-2-(methylthio)-7*H*-pyrrolo[2,3-*d*]pyrimidine (15).

Sodium hydride (60% dispersion in mineral oil, 0.1 g, 2.5 mmol) was slowly added to a solution of 4-chloro-2-(methylthio)-7*H*-pyrrolo[2,3-*d*]pyrimidine **11** (0.19 g, 1 mmol) in anhydrous acetonitrile

freshly distilled (5 mL) and the mixture was stirred at room temperature for 20 min. Then 4-fluorobenzyl chloride (0.14 g, 1 mmol) solved in anhydrous acetonitrile (5 mL) was added dropwise. The mixture was heated at 50 °C for 2h, then cooled to room temperature and filtered to eliminate the little amount of solid obtained. The solution was then evaporated under reduced pressure and the crude was purified by column chromatography (Florisil®, 100-200 mesh), using diethyl ether as the eluent to afford pure 4-chloro-7-(4-fluorobenzyl)-2-(methylthio)-7*H*-pyrrolo[2,3-*d*]pyrimidine **15** as light yellow solid (36%). Mp: 99-100 °C. ^{1}H NMR ($CDCl_3$): δ 2.65 (s, 3H, SCH_3), 5.36 (s, 2H, CH_2N), 6.53 (d, *J* = 3.6, 1H, H-5), 6.96-7.04 and 7.14-7.24 (2m, 5H, 4Ar + H-6). MS: *m/z* $[M+1]^+$ 309. Anal. calcd. for $C_{14}H_{11}N_3ClFS$, C 54.63, H 3.60, N 13.65, S 10.42, found C 54.41, H 3.69, N 13.42, S 10.15.

4.1.9 General procedure for the synthesis compounds 8d-j.

The suitable amine (5 mmol) was added to a solution of 4-chloro-7-(4-fluorobenzyl)-2-(methylthio)-7*H*-pyrrolo[2,3-*d*]pyrimidine **15** (0.31 g, 1 mmol) in DMSO (5 mL) and the mixture was heated at 90-130 °C (the temperature depended on the boiling point of the amine) for 3-5h, monitoring by TLC the product formation. Then the mixture was cooled to room temperature, poured in ice-water (50 mL), extracted with CH_2Cl_2 (3 x 20 mL), dried on $MgSO_4$, filtered and concentrated under reduced pressure. The crude was purified by column chromatography (Florisil®, 100-200 mesh), using $CHCl_3$ as the eluent to afford the pure products.

4.1.9.1 *N*-Butyl-7-(4-fluorobenzyl)-2-(methylthio)-7*H*-pyrrolo[2,3-*d*]pyrimidin-4-amine (8d). Yield: 42%, (yellow oil). ^{1}H NMR ($CDCl_3$): δ 0.89 (t, *J* = 7.2, 3H, CH_3), 1.37 (sx, *J* = 7.2, 2H, $\underline{CH_2}CH_3$), 1.59 (quint, *J* = 7.2, 2H, $\underline{CH_2}CH_2CH_3$), 2.52 (s, 3H, SCH_3), 3.53 (q, *J* = 7.2, 2H, CH_2NH), 5.04 (br s, 1H, NH disappears with D_2O), 5.21 (s, 2H, CH_2N), 6.22 (d, *J* = 3.6, 1H, H-5), 6.65 (d, *J* = 3.6, 1H, H-6), 6.84-6.94 and 7.07-7.21 (2m, 4H Ar). IR (KBr) cm^{-1}: 3382 (NH). ^{13}C NMR (MeOD): δ 170.01, 162.67, 154.48, 147.83, 132.42, 130.45, 125.95, 115.11, 103.01, 101.64,

50.49, 43.71, 30.87, 20.23, 14.82, 14.02. MS: *m/z* $[M+1]^+$ 345. Anal. calcd. for $C_{18}H_{21}N_4FS$, C 62.76, H 6.15, N 16.27, S 9.31, found C 62.58, H 6.45, N 16.21, S 9.08.

4.1.9.2 7-(4-Fluorobenzyl)-2-(methylthio)-4-pyrrolidin-1-yl-7*H*-pyrrolo[2,3-*d*]pyrimidine (8e). Yield: 52%, (yellow solid), mp 149-150 °C. ^{1}H NMR ($CDCl_3$): δ 1.86-2.00 (m, 4H, $2CH_2$ pyrr.), 2.51 (s, 3H, SCH_3), 3.66-3.78 (m, 4H, $2CH_2N$ pyrr.), 5.22 (s, 2H, CH_2N), 6.39 (d, *J* = 3.4, 1H, H-5), 6.61 (d, *J* = 3.4, 1H, H-6), 6.83-6.96 and 7.07-7.21 (2m, 4H Ar). ^{13}C NMR (MeOD): δ 167.66, 162.67, 155.30, 151.11, 132.42, 130.45, 123.66, 115.11, 110.00, 101.76, 65.59, 50.49, 45.92, 14.82. MS: *m/z* $[M+1]^+$ 343. Anal. calcd. for $C_{18}H_{19}N_4FS$, C 63.13, H 5.59, N 16.36, S 9.36, found C 63.25, H 5.69, N 16.27, S 9.06.

4.1.9.3 7-(4-Fluorobenzyl)-2-(methylthio)-4-piperidin-1-yl-7*H*-pyrrolo[2,3-*d*]pyrimidine (8f). Yield: 46%, (yellow solid), mp 73-74 °C. ^{1}H NMR ($CDCl_3$): δ 1.51-1.72 (m, 6H, $3CH_2$ pip.), 2.50 (s, 3H, SCH_3), 3.74-3.88 (m, 4H, $2CH_2N$ pip.), 5.23 (s, 2H, CH_2N), 6.34 (d, *J* = 3.6, 1H, H-5), 6.65 (d, *J* = 3.6, 1H, H-6), 6.83-6.98 and 7.08-7.21 (2m, 4H Ar). ^{13}C NMR (MeOD): δ 167.66, 162.67, 155.30, 151.11, 132.42, 130.45, 123.66, 115.11, 110.00, 101.76, 50.49, 48.07, 25.08, 23.42, 14.82. MS: *m/z* $[M+1]^+$ 357. Anal. calcd. for $C_{19}H_{21}N_4SF$, C 64.02, H 5.94, N 15.72, S 9.00, found C 64.24, H 5.94, N 15.70, S 9.07.

4.1.9.4 7-(4-Fluorobenzyl)-2-(methylthio)-4-morpholin-4-yl-7*H*-pyrrolo[2,3-*d*]pyrimidine (8g). Yield: 51%, (yellow solid), mp 115-116 °C. ^{1}H NMR ($CDCl_3$): δ 2.50 (s, 3H, SCH_3), 3.75 (t, *J* = 5.4, 4H, 2 CH_2N morph.), 3.87 (t, *J* = 5.4, 4H, 2 CH_2O morph.), 5.24 (s, 2H, CH_2N), 6.33 (d, *J* = 3.6, 1H, H-5), 6.69 (d, *J* = 3.6, 1H, H-6), 6.84-6.98 and 7.06-7.23 (2m, 4H Ar). ^{13}C NMR (MeOD): δ 168.25, 162.67, 153.43, 151.84, 132.42, 130.45, 123.66, 115.11, 108.99, 101.76, 50.49, 49.09, 26.01, 14.82. MS: *m/z* $[M+1]^+$ 359. Anal. calcd. for $C_{18}H_{19}N_4FSO$, C 60.32, H 5.34, N 15.63, S 8.95, found C 60.15, H 5.44, N 15.63, S 8.70.

4.1.9.5 *N*-Benzyl-7-(4-fluorobenzyl)-2-(methylthio)-7*H*-pyrrolo[2,3-*d*]pyrimidin-4-amine (8h). Yield: 36%, (yellow solid), mp 95-96 °C. ^{1}H NMR ($CDCl_3$): δ 2.51 (s, 3H, SCH_3), 4.76 (d, *J* = 5.8, 2H, $\underline{CH_2}NH$), 5.22 (s, 2H, CH_2N), 6.17 (d, *J* = 3.6, 1H, H-5), 6.62 (d, *J* = 3.4, 1H, H-6), 6.83-6.97

and 7.07-7.38 (2m, 9H Ar), 7.73 (br s, 1H, NH disappears with D_2O). IR (KBr) cm^{-1}: 3228 (NH). ^{13}C NMR (MeOD): δ 169.91, 162.67, 153.45, 147.86, 139.85, 132.42, 130.45, 128.43, 127.59, 126.92, 125.95, 115.11, 103.57, 101.64, 50.49, 43.38, 14.82. MS: *m/z* $[M+1]^+$ 379. Anal. calcd. for $C_{21}H_{19}N_4FS$, C 66.64, H 5.06, N 14.80, S 8.47, found C 66.52, H 5.18, N 14.64, S 8.17.

4.1.9.6 7-(4-Fluorobenzyl)-2-(methylthio)-*N*-(2-phenylethyl)-7*H*-pyrrolo[2,3-*d*]pyrimidin-4-amine (8i). Yield: 37%, (brown solid), mp 61-68 °C. ^1H NMR ($CDCl_3$): δ 2.56 (s, 3H, SCH_3), 2.92 (t, *J* = 6.8, 2H, CH_2Ar), 3.81 (q, *J* = 6.8, 2H, $\underline{CH_2}NH$), 5.07 (br s, 1H, NH disappears with D_2O), 5.21 (s, 2H, CH_2N), 6.15 (d, *J* = 3.4, 1H, H-5), 6.64 (d, *J* = 3.4, 1H, H-6), 6.83-6.98 and 7.06-7.33 (2m, 9H Ar). IR (KBr) cm^{-1}: 3317 (NH). ^{13}C NMR (MeOD): δ 170.01, 162.67, 154.48, 147.83, 139.08, 132.42, 130.45, 129.19, 128.83, 126.13, 125.95, 115.11, 103.01, 101.64, 50.49, 43.75, 35.64, 14.82. MS: *m/z* $[M+1]^+$ 393. Anal. calcd. for $C_{22}H_{21}N_4FS$, C 67.32, H 5.39, N 14.27, S 8.17, found C 67.34, H 5.60, N 14.36, S 8.00.

4.1.9.7 *N*-[2-(4-Chlorophenyl)ethyl]-7-(4-fluorobenzyl)-2-(methylthio)-7*H*-pyrrolo[2,3-*d*]pyrimidin-4-amine (8j). Yield: 31%, (yellow solid), mp 141-143 °C. ^1H NMR ($CDCl_3$): δ 2.55 (s, 3H, SCH_3), 2.90 (t, *J* = 6.8, 2H, CH_2Ar), 3.83 (q, *J* = 6.8, 2H, $\underline{CH_2}NH$), 5.15 (br s, 1H, NH disappears with D_2O), 5.25 (s, 2H, CH_2N), 6.18 (d, *J* = 3.4, 1H, H-5), 6.67 (d, *J* = 3.4, 1H, H-6), 6.85-7.01 and 7.10-7.37 (2m, 8H Ar). IR (KBr) cm^{-1}: 3310 (NH). ^{13}C NMR (MeOD): δ 170.01, 162.67, 154.48, 147.83, 136.26, 132.64, 132.42, 130.45, 130.05, 129.35, 125.95, 115.11, 103.01, 101.64, 50.49, 43.75, 35.64, 14.82. MS: m/z $[M+1]^+$ 428. Anal. calcd. for $C_{22}H_{20}N_4ClFS$, C 61.89, H 4.72, N 13.12, S 7.51, found C 61.67, H 4.57, N 13.10, S 7.33.

4.2 Molecular Modeling

4.2.1 Proteins Preparation. Crystal structures of c-Src in complex with **11V** (PDB code: 4O2P) has been previously published by our group and used for the present study [11]. After removal of bound ligand, both chain A and chain B were prepared by using the Protein Preparation Wizard [36] workflow, from Schrödinger Suite. The ionization and tautomeric states of His, Asp, Glu, Arg and

Lys were adjusted to match a pH of 7.4. Next, optimization of the hydrogen-bonding network was obtained by reorienting hydroxyl and thiol groups, amide groups of Asn and Gln, and His ring. Finally, the systems were refined by running a restrained minimization (OPLS3 force field) which was stopped when RMSD of heavy atoms reached 0.30 Å, the specified limit by default.

4.2.2 Ligand Preparation. All compounds were drawn and minimized using Maestro 10.4 and Macromodel 11.0 (Schrödinger suite) [37], respectively. Furthermore, Ligprep 3.6 [37] was used to predict ionization and tautomeric states for the ligands using a pH of 7±0.5.

4.2.3 Docking Studies. Docking simulations were performed using the Glide program [36] within the ATP binding sites of Src. The prepared protein systems were used to generate the receptor grids, and no scaling was done for van der Waals radii of nonpolar receptor atoms. A grid box of default size was centered on the X-ray ligand. No constraints were included during grid generation while the rotation of the hydroxyl groups was allowed. After grid preparation, compounds were flexibly docked and scored using the Glide standard-precision (SP) mode, treating the proteins as rigid. Docking experiments were performed using 0.80 factor to scale van der Waals radii of the nonpolar ligand atoms with partial atomic charge less than 0.15.

4.2.4 MM-GBSA. For the MM-GBSA analysis Prime 4.2 [37] program has been used. The binding free energy (ΔG_{bind}) for each compound was calculated using the following equation:

Eq 1. $$\Delta G_{bind} = \Delta G_{MM} + \Delta G_{sovl} + \Delta G_{SA}$$

where ΔG_{MM} is the difference in the minimized energies between the Src-ligands complexes and the sum of the energies of the apo enzyme and the free compound. ΔG_{solv} is the difference in the GBSA solvation energy of the Src-ligand complexes and the sum of the solvation energies for the unbound enzyme and inhibitor. ΔG_{SA} is the difference in surface area energies for the complexes and the sum of the surface area energies for the apo-Src and unbound inhibitor.

5. Biological Assays

5.1 *In vitro* kinase inhibition assays

Chemicals were purchased from Sigma-Aldrich, pure ATP was from Promega and P33-g-ATP was from Hartman Analytic. Recombinant full length, HIS_6-tagged Src and Fyn were purchased from Merk Millipore; recombinant GST tagged, C-terminal fragment (696-end), EGFR was also from Merk Millipore; recombinant GST-HIS_6 C-terminal fragment (544-976) Kit was purchased from ProQinase.

Assays conditions. Fyn and Src reactions were performed in 50 mM MOPS/NaOH, pH 7.0, 0.1 mM EDTA, 0.0013% or 0.00087% NP40 respectivelly, 0.1 mM Na_3VO_4, 10% DMSO, 3 mM $MnCl_2$/$MgCl_2$, 100 μM ATP/[γ-33P]ATP, 250 μM of the Src substrate peptide KVEKIGEGTYGVVYK, and 30 ng active enzyme.

Kit and Flt3 reaction were performed in 60 mM HEPES/NaOH pH 7.5, 0.0013% NP40, 3 mM Na_3VO_4, 10% DMSO, 3 mM $MgCl_2$/$MnCl_2$, 1.2 mM DTT, 50 mg/ml PEG6.000, 20 μM and 2 μM ATP/[γ-33P]ATP respectively. For only Kit reaction, 100 μM HER2 substrate peptide GGMEDIYFEFMGGKKK and 50 ng of active enzyme were used, while, for Flt3 reaction, 50 μM peptide substrate KVEKIGEGTYGVVYK and 50 ng of enzyme were used.

EGFR reaction were performed in 20 mM HEPES/NaOH pH 7.5, MOPS/NaOH, pH 7.0, 0.1 mM EDTA, 0.01% NP40, 5% glycerol, 0.1 mM 2-mercaptoethanol, 1 mg/ml BSA, 10 mM $MnCl_2$/$MgCl_2$, 0.8M $(NH_4)SO_4$, 16 μM ATP/[γ-33P]ATP, 400 μM angiotensin 2 (substrate) and 35 ng of active enzyme.

To avoid plastic adsorption of enzymes and peptide, all reactions were performed using protein low-binding tubes (LoBind, Eppendorf). All reactions were performed in 10 ml at 30 °C for 10 min. Reactions were stopped by adding 5 ml of phosphoric acid 0.5%. Aliquots (10 mL) were transferred on P30 Filtermat (PerkinElmer), washed five times with 75 mM phosphoric acid for 5 min and once with acetone for 4 min. The filter was dried and transferred to a sealable plastic bag, and

scintillation cocktail (4 mL) was added. Spotted reactions were read in a scintillation counter (Trilux, PerkinElmer).

ID_{50} values were obtained according to Equation (2), where *v* is the measured reaction velocity, V is the apparent maximal velocity in the absence of inhibitor, I is the inhibitor concentration, and ID_{50} is the 50% inhibitory dose.

Eq. 2 $v = V/\{1+(I/ID_{50})\}$

5.2 Cell viability

In vitro experiments were carried out using the Glioblastoma cell line U87 MG. Cells were purchased from American Type Culture Collection (ATCC, Manassas, VA, USA) and were cultured in Eagle's Minimum Essential Medium (EMEM) supplemented with 10% FBS, 2 mM L-glutamine and 10000 units/mL Penicillin/Streptomycin at 37 °C in 5% CO_2 atmosphere.

Briefly, 2.5×10^4 U87 MG cells were plated in 12-well plates and incubated with compounds in DMSO at increasing concentrations (0.1, 1.0, 10 and 100 µM) for 24, 48 and 72h at 37 °C in 5% v/v CO_2. Cell number and viability were evaluated using Z2 Coulter Counter (Beckman Coulter). IC_{50} (drug concentration that determined the 50% of growth inhibition) was calculated by GraphPad Prism 6.0 software using the best fitting sigmoid curve.

Acknowledgments

Lead Discovery Siena s.r.l. is acknowledged for financial support.

References

[1] J.M. Kaplan, H.E. Varmus, J.M. Bishop, The src protein contains multiple domains for specific attachment to membranes, Mol. Cell. Biol. 10 (1990) 1000-1009.

[2] L.C. Kim, L. Song, E.B. Haura, Src kinases as therapeutic targets for cancer, Nat. Rev. Clin. Oncol. 6 (2009) 587-595.

[3] S. Schenone, F. Manetti, M. Botta, SRC inhibitors and angiogenesis, Curr. Pharm. Des. 13 (2007), 2118-2128.

[4] J. de Groot, V. Milano, Improving the prognosis for patients with glioblastoma: the rationale for targeting Src, J. Neurooncol. 95 (2009) 151-163.

[5] R. Roskoski Jr., Src protein-tyrosine kinase structure, mechanism, and small molecule inhibitors, Pharmacol. Res. 94 (2015) 9-25.

[6] F. Musumeci, S. Schenone, C. Brullo, M. Botta, An update on dual Src/Abl inhibitors, Future Med. Chem. 4 (2012) 799-822.

[7] C. Gambacorti-Passerini, A. Aroldi, N. Cordani, R. Piazza, Chronic myeloid leukemia: Second-line drugs of choice, Am. J. Hematol. 91 (2016) 67-75.

[8] S. Schenone, M. Radi, F. Musumeci, C. Brullo, M. Botta, Biologically driven synthesis of pyrazolo[3,4-*d*]pyrimidines as protein kinase inhibitors: an old scaffold as a new tool for medicinal chemistry and chemical biology studies, Chem. Rev. 114 (2014) 7189-7238.

[9] S. M. El-Moghazy, R. F. George, E. E. A. Osman, A. A. Elbatrawy, M. Kissova, A. Colombo, E. Crespan, G. Maga, Novel pyrazolo[3,4-*d*]pyrimidines as dual Src-Abl inhibitors active against mutant form of Abl and the leukemia K-562 cell line, Eur. J. Med. Chem. 123 (2016) 1-13.

[10] M. Radi, C. Tintori, F. Musumeci, C. Brullo, C. Zamperini, E. Dreassi, A.L. Fallacara, G. Vignaroli, E. Crespan, S. Zanoli, I. Laurenzana, Design, synthesis, and biological evaluation of pyrazolo[3,4-*d*]pyrimidines active *in vivo* on the Bcr-Abl T315I mutant, J. Med. Chem. 56 (2013) 5382-5394.

[11] C. Tintori, A.L. Fallacara, M. Radi, C. Zamperini, E. Dreassi, E. Crespan, G. Maga, S. Schenone, F. Musumeci, C. Brullo, A. Richters, F. Gasparrini, A. Angelucci, C. Festuccia, S. Delle Monache, D. Rauh, M. Botta, Combining X-ray crystallography and

molecular modeling toward the optimization of pyrazolo[3,4-*d*]pyrimidines as potent c-Src inhibitors active *in vivo* against neuroblastoma, J. Med. Chem. 58 (2015) 347-361.

[12] C. Tintori, G. La Sala, G. Vignaroli, L. Botta, A.L. Fallacara, F. Falchi, M. Radi, C. Zamperini, E. Dreassi, L. Dello Iacono, D. Orioli, G. Biamonti, M. Garbelli, A. Lossani, F. Gasparrini, T. Tuccinardi, I. Laurenzana, A. Angelucci, G. Maga, S. Schenone, C. Brullo, F. Musumeci, A. Desogus, E. Crespan, M. Botta, Studies on the ATP binding site of Fyn kinase for the identification of new inhibitors and their evaluation as potential agents against tauopathies and tumors, J. Med. Chem. 58 (2015) 4590-4609.

[13] M.E. Flanagan, T.A. Blumenkopf, W.H. Brissette, M.F. Brown, J.M. Casavant, C. Shang-Poa, J.L. Doty, E.A. Elliott, M.B. Fisher, M. Hines, C. Kent, E.M. Kudlacz, B.M. Lillie, K.S. Magnuson, S.P. McCurdy, M.J. Munchhof, B.D. Perry, P.S. Sawyer, T.J. Strelevitz, C. Subramanyam, J. Sun, D.A. Whipple, P.S. Changelian, Discovery of CP-690,550: a potent and selective Janus kinase (JAK) inhibitor for the treatment of autoimmune diseases and organ transplant rejection, J. Med. Chem. 53 (2010) 8468-8484.

[14] A. Deisseroth, E. Kaminskas, J. Grillo, W. Chen, H. Saber, H.L. Lu, M.D. Rothmann, S. Brar, J. Wang, C. Garnett, J. Bullock, L.B. Burke, A. Rahman, R. Sridhara, A. Farrell, R. Pazdur, U.S. Food and Drug Administration approval: ruxolitinib for the treatment of patients with intermediate and high-risk myelofibrosis, Clin. Cancer Res. 18 (2012) 3212-3217.

[15] A.J. Gonzales, J.B. Bowman, G.J. Fici, M. Zhang, D.W. Mann, M. Mitton-Fry, Oclacitinib (APOQUEL(®)) is a novel Janus kinase inhibitor with activity against cytokines involved in allergy, J. Vet. Pharmacol. Ther. 37 (2014) 317-324.

[16] D.M. Schwartz, M. Bonelli, M. Gadina, J.J. O'Shea, Type I/II cytokines, JAKs, and new strategies for treating autoimmune diseases, Nat. Rev. Rheumatol. 12 (2016) 25-36.

[17] P. Traxler, P.R. Allegrini, R. Brandt, J. Brueggen, R. Cozens, D. Fabbro, K. Grosios, H.A. Lane, P. McSheehy, J. Mestan, T. Meyer, C. Tang, M. Wartmann, J. Wood, G.

Caravatti, AEE788: a dual family epidermal growth factor receptor/ErbB2 and vascular endothelial growth factor receptor tyrosine kinase inhibitor with antitumor and antiangiogenic activity, Cancer Res. 64 (2004) 4931-4941.

[18] A. Valverde, J. Peñarando, A. Cañas, L.M. López-Sánchez, F. Conde, V. Hernández, E. Peralbo, C. López-Pedrera, J. de la Haba-Rodríguez, E. Aranda, A. Rodríguez-Ariza, Simultaneous inhibition of EGFR/VEGFR and cyclooxygenase-2 targets stemness-related pathways in colorectal cancer cells, PLoS One. 10 (2015) e0131363.

[19] a) https://clinicaltrials.gov/ct2/show/NCT00107237?term=NCT00107237&rank=1 (accessed 10.07.16).

b) https://clinicaltrials.gov/ct2/show/NCT00116376?term=NCT00116376&rank=1 (accessed 10.07.16).

[20] T.A. Yap, M.I. Walton, L.K. Hunter, M. Valenti; B.A. de Haven, P.D. Eve, R. Ruddle, S.P. Heaton, A. Henley, L. Pickard, G. Vijayaraghavan, J.J.Caldwell, N.T. Thompson, W. Aherne, F.I. Raynaud, S.A. Eccles, P. Workman, I. Collins, M.D. Garrett, Preclinical pharmacology, antitumor activity, and development of pharmacodynamic markers for the novel, potent AKT inhibitor CCT128930, Mol. Cancer Ther. 10 (2011) 360-371.

[21] M. Addie, P. Ballard, D. Buttar, C. Crafter, G. Currie, B.R. Davies, J. Debreczeni, H. Dry, P. Dudley, R. Greenwood, P.D. Johnson, J.G. Kettle, C. Lane, G. Lamont, A. Leach, R.W. Luke, J. Morris, D. Ogilvie, K. Page, M. Pass, S. Pearson, L. Ruston, Discovery of 4-amino-N-[(1S)-1-(4-chlorophenyl)-3-hydroxypropyl]-1-(7*H*-pyrrolo[2,3-*d*]pyrimidin-4-yl)piperidine-4-carboxamide (AZD5363), an orally bioavailable, potent inhibitor of Akt kinases, J. Med. Chem. 56 (2013) 2059-2073.

[22] https://clinicaltrials.gov/ct2/results/displayOpt?flds=a&flds=b&flds=f&flds=k&submit_fld_opt=on&term=azd5363&show_flds=Y (accessed 12.07.16).

[23] J.M. Hatcher, J. Zhang, H.G. Choi, G. Ito, D.R. Alessi, N.S. Gray, Discovery of a pyrrolopyrimidine (JH-II-127), a highly potent, selective, and brain penetrant LRRK2 inhibitor, ACS Med. Chem. Lett. 6 (2015) 584-589.

[24] S.T. Murphy, G. Alton, S. Bailey, S.M. Baxi, B.J. Burke, T.A. Chappie, J. Ermolieff, R. Ferre, S. Greasley, M. Hickey, J. Humphrey, N. Kablaoui, J. Kath, S. Kazmirski, M. Kraus, S. Kupchinsky, J. Li, L. Lingardo, M.A. Marx, D. Richter, S.P. Tanis, K. Tran, W. Vernier, Z. Xie, M.J. Yin, X.H. Yu, Discovery of novel, potent, and selective inhibitors of 3-phosphoinositide-dependent kinase (PDK1), J. Med. Chem. 54 (2011) 8490-8500.

[25] J. Le Brazidec, A. Pasis, B. Tam, C. Boykin, D. Wang, D.J. Marcotte, G. Claassen, J. Chong, J. Chao, J. Fan, K. Nguyen, L. Silvian, L. Ling, L. Zhang, M. Choi, M. Teng, N. Pathan, S. Zhao, T. Li, A. Taveras, Structure-based design of 2,6,7-trisubstituted-7*H*-pyrrolo[2,3-*d*]pyrimidines as Aurora kinases inhibitors, Bioorg. Med. Chem. Lett. 22 (2012) 4033-4037.

[26] A. Gangjee, S. Kurup, M.A. Ihnat, J.E. Thorpe, B. Disch, N4-Aryl-6-substituted phenylmethyl-7*H*-pyrrolo[2,3-*d*]pyrimidines-2,4-diamines as receptor tyrosine kinase inhibitors, Bioorg. Med. Chem. 20 (2012) 910-914.

[27] A. Gangjee, O.A. Namjoshi, J. Yu, M.A. Ihnat, J.E. Thorpe, L.C. Bailey-Downs, N2-Trimethylacetyl substituted and unsubstituted-N4-phenylsubstituted-6-(2-pyridin-2-ylethyl)-7*H*-pyrrolo[2,3-*d*]pyrimidines-2,4-diamines: Design, cellular receptor tyrosine kinase inhibitory activities and *in vivo* evaluation as antiangiogenic, antimetastatic and antitumor agents, Bioorg. Med. Chem. 21 (2013) 1312-1323.

[28] X. Zhao, W. Huang, Y. Wang, M. Xin, Q. Jin, J. Cai, F. Tang, Y. Zhao, H. Xiang, Discovery of novel Bruton's tyrosine kinase (BTK) inhibitors bearing a pyrrolo[2,3-*d*]pyrimidine scaffold, Bioorg. Med. Chem. 23 (2015) 891-901.

[29] A. Laurent, Y. Rose, Preparation of pyrrolopyrimidinamines as protein kinase inhibitors and therapeutic uses thereof. 2015 WO 2015077866.

[30] S.J. Kaspersen, J. Han, K.G. Nørsett, L. Rydså, E. Kjøbli, S. Bugge, G. Bjørkøy, E. Sundby, B.H. Hoff, Identification of new 4-N-substituted 6-aryl-7*H*-pyrrolo[2,3-*d*]pyrimidine-4-amines as highly potent EGFR-TK inhibitors with Src-family activity, Eur. J. Pharm. Sci. 59 (2014) 69-82.

[31] S. Dincer, K.T. Cetin, A. Onay-Besikci, S. Olgen, Synthesis, biological evaluation and docking studies of new pyrrolo[2,3-*d*]pyrimidine derivatives as Src family-selective tyrosine kinase inhibitors, J. Enzyme Inhib. Med. Chem. 28 (2013) 1080-1087.

[32] B.R. Baker, J.P. Joseph, R.E. Schaub, Synthetic studies. I. Synthesis of 6-dimethylaminopurine, a hydrolytic fragment, J. Org. Chem. 19 (1954), 631-637.

[33] C.W. Noell, R.K. Robins, Aromaticity in heterocyclic systems. II. The application of N.M.R. in a study of the synthesis and structure of certain imidazo[1,2-*c*]pyrimidines and related pyrrolo[2,3-*d*]pyrimidines. J. Heterocyclic Chem. 1 (1964) 34-41.

[34] W. Xu, A. Doshi, M. Lei, M.J. Eck, S.C. Harrison, Crystal structure of c-Src reveal features of its autoinhibitory mechanism. Mol. Cell. 3 (1999) 629-638.

[35] J.C. Williams, A. Weijland, S. Gonfloni, A. Thompson, S.A. Courtneidge, G. Superti-Furga, R.K. Wierenga, The 2.35 A crystal structure of the inactivated form of chiken Src: a dynamic molecule with multiple regulatory interactions. J. Mol. Biol. 274 (1997) 757-775.

[36] Glide, version 6.9, Schrödinger, LLC, New York, 2015.

[37] Schrödinger Suite 2015-4 Protein Preparation Wizard; Epik version 3.4, LLC, New York, 2015; Prime version 4.2, LLC, New York, 2015.

[38] E. Ceccherini, P. Indovina, C. Zamperini, E. Dreassi, N. Casini, O. Cutaia, I.M. Forte, F. Pentimalli, L. Esposito, M.S. Polito, S. Schenone, M. Botta, A. Giordano, Src family kinase inhibition through a new pyrazolo[3,4-*d*]pyrimidine derivative as a feasible approach for glioblastoma treatment. J. Cell. Biochem. 116 (2015) 856-863.

List of captions

Fig. 1. Structures of dual Src/Abl inhibitors approved or in clinical trials for solid or hematologic malignancies.

Fig. 2. In house library of pyrazolo[3,4-*d*]pyrimidines **1**.

Fig. 3. Pyrrolo[2,3-*d*]pyrimidine kinase inhibitors.

Fig. 4. General structure of pyrrolo[2,3-*d*]pyrimidines **8**.

Fig 5. *Left)* Schematic representation of **11V** ligand's interactions within the ATP-binding site of c-Src; *Right)* Binding mode of **11V** in 4O2P crystal structure: panel A and panel B show chain A and chain B, respectively. DFG-motif and Glu310 are displayed as sticks. Hydrogen bonds are reported as yellow dashes.

Fig 6. Best predicted docking poses of compounds **8b** (orange, panel A), **8h** (deep teal, panel B) and **8e** (pale green, panel C) within the ATP binding site of 4O2P crystal structure chain B.

Fig. 7. Viability of U87 cell line evaluated at 72h is reported for the most active compound **8h** and for **8b** and **8e** as examples of less active compounds of each series.

Table 1: Structures and inhibitory activity of compounds **8a-j**.

Scheme 1. Synthetic route for the preparation of **8a-c**. Reagents and conditions: (i) Chloroacetaldehyde (50% aq. solution), AcONa, H_2O, MW 100 W, 80 °C, 2 min. (ii) $POCl_3$, TEA, 130 °C, 4h. (iii) NaH, anhyd. DMF, 0 °C, 20 min, then 2-bromo-1-phenylethanone, from 0 °C to rt, 18h. (iv) $NaBH_4$, THF, H2O, 0 °C, then rt, 3h. (v) $POCl_3$/DMF, CH_2Cl_2, reflux, 8h. (vi) Method A: anilines, abs. EtOH, reflux, 5h (to obtain compounds **8a,b**); Method B: benzylamine, anhyd. toluene, rt, 24h (to obtain compound **8c**).

Scheme 2. Synthetic route for the preparation of **8d-j**. Reagents and conditions: (i), NaH, anhyd. CH_3CN, 4-fluorobenzyl chloride, 50 °C, 2h. (ii) amines, DMSO, 90-130 °C, 3-5h.

Identification of new pyrrolo[2,3-*d*]pyrimidines as Src tyrosine kinase inhibitors *in vitro* active against Glioblastoma

Highlights

- The synthesis of 10 new pyrrolo[3,4-*d*]pyrimidines derivatives is reported
- Molecular modeling studies showed pyrrolo-pyrimidine derivatives can efficiently bind the ATP-binding site of c-Src kinase
- The synthesized compounds have been tested on a small panel of kinases
- One hit compound demonstrated a very interesting cytotoxic effect against U87 Glioblastoma cell line